Journal of Molecular Structure 1103 (2016) 45–55

Contents lists available at ScienceDirect

Journal of Molecular Structure

journal homepage: http://www.elsevier.com/locate/molstruc

Synthesis and characterization of 3-aminoquinoline derivatives and studies of photophysicochemical behaviour and antimicrobial activities

Gulay Zengin [a, *], Ali Muayad Nafea Al Kawaz [a], Huseyin Zengin [a], Adem Mert [a], Bedia Kucuk [b]

[a] Department of Chemistry, Faculty of Science and Literature, Gaziantep University, Gaziantep, 27310, Turkey
[b] Department of Biology, Faculty of Science and Literature, Kahramanmaras Sutcu Imam University, Kahramanmaras, 46100, Turkey

ARTICLE INFO

Article history:
Received 13 July 2015
Received in revised form
10 September 2015
Accepted 12 September 2015
Available online 14 September 2015

Keywords:
Naphthalene
Quinoline derivatives
Antimicrobial activity
Photoluminescence

ABSTRACT

A series of 3-aminoquinoline derivatives were synthesized, where their chemical structures were confirmed by various analytical techniques, such as, Elemental Analysis, Nuclear Magnetic Resonance Spectroscopy (^{1}H and ^{13}C NMR), Liquid Chromatography-Mass-Mass Spectroscopy (LC-MS-MS), Ultraviolet–Visible Spectroscopy (UV–Vis), Fourier Transform Infrared Spectroscopy (FTIR) and Photoluminescence (PL). The quinoline ring core, typical of aminoquinolines, and a naphthalene group was combined to devise (4-alkyl-1-naphthyl)-quinolin-3-ylamide derivatives. These derivatives were designed and synthesized in light of the chemical and biological profiles of these important subunits. All the compounds were evaluated for their *in vitro* antibacterial and antifungal activities by the paper disc diffusion method with Gram-positive *Bacillus subtilis*, *Bacillus megaterium* and *Staphylococcus aureus*, Gram-negative *Enterobacter aerogenes*, *Eschericha coli*, *Klebsiella pneumoniae* and *Pseudomonas aeruginosa* and yeasts *Candida albicans*, *Saccharomyces cerevisiae* and *Yarrovia lipolytica*. These compounds showed antimicrobial activities against Gram-positive and Gram-negative bacteria and several yeasts, and thus their activity was not restricted to any particular type of microorganism.

1. Introduction

The basis of drug design is to develop chemical compounds having maximum medicinal applications and minimum toxicological effects. Both naphthalene and quinoline are important structural units, commonly used in antimicrobial therapeutics. Popular drugs containing naphthalene include the β-blocker drug propranolol used for heart disease, and antimicrobial agents, such as, naftifine and nafcillin, which have antifungal and antibacterial properties, respectively; nafcillin is a penicillin-type antibacterial drug, that has been structurally modified via naphthalene replacement with quinoline, in an effort to overcome drug resistance, specifically by action on the β-lactamase enzyme of *Staphylococci* [1].

Quinoline consists of a benzene ring fused to a pyridine ring, thus is a heterocyclic aromatic compound, and very much resembles the structure of naphthalene. Thus, it is not surprising to find work in the literature involving these two quinoline and naphthalene moieties, where these structural cores have been interchanged, or derivatizations have been made. Quinoline-bearing compounds are naturally present in plants. Quinoline derivatives are varied, and have a wide range of applications, in particular, are used as antibiotics against a variety of bacteria that have acquired resistance to regular antibiotics. Quinoline derivatives, like other types of heterocyclic compounds, possess anticancer and anti-HIV properties [2]. Further, a study showed quinoline cannabinoid derivatives having analgesic activity via selective agonist activity for cannabinoid CB_2 receptors [3]. The literature reveals a study on quinoline and naphthalene derivatives evaluated for antimycobacterial properties [4]. Here the structural design for derivatization was influenced by the drugs mefloquine and TMC207, where mefloquine is a quinoline analogue, and TMC207 bears both the naphthalene and quinoline subunits [5].

While both naphthalene and quinoline derivatives have been shown to have an important role in medicinal chemistry, providing

* Corresponding author.
E-mail address: gzengin@gantep.edu.tr (G. Zengin).

http://dx.doi.org/10.1016/j.molstruc.2015.09.016
0022-2860/

a wide variety of bioactivities, such as, antibiotic and anticancer properties [6–9], a common feature of these structures is that they have been shown to have antiinflammatory and analgesic effects. In this context, the study herein presents work on novel compounds bearing both these two structural cores for possible antiinflammatory and analgesic effects, in the development of effective therapeutic compounds of nonsteroidal nature.

We have already reported work on the synthesis of new naphthoyl sulfonamides [10], where biological evaluations and photochemical properties were presented. In this study, new 3-aminoquinoline derivatives were synthesized and screened for antimicrobial activity to assist in the development of antibiotic drugs with analgesic and anti-inflammatory properties. Fluorescence properties of the derivatives were also investigated, as they may bear good fluorescence, and have potential in optical technology for microscopic diagnostics.

2. Materials and method

2.1. Materials and reagents

Solvents and reagents were purchased from Sigma Aldrich and Merck Chemical companies, and used without further purification, unless reactions called for dry conditions. The solvents used were diethyl ether, ethanol, methanol, tetrahydrofuran (THF), *N,N*-dimethylformamide (DMF), dichloromethane (DCM), 1,2-dichloroethane, diethylene glycol, petroleum ether, ethyl acetate and hexane. The reagents used were ethylmagnesium bromide (3.0 M), propylmagnesium chloride (2.0 M), 1-cyanonaphthalene, diphenylcarbamoyl chloride, oxalyl chloride, 1-ethylnaphthalene, 3-aminoquinoline, anhydrous aluminum chloride, semicarbazide hydrochloride, 4-methyl morpholine (*N*-ethyl morpholine, NEM), 9,10-diphenylanthracene and hydrochloric acid.

2.2. Instrumentation and conditions

Melting points of compounds were obtained by a SRS Model melting point apparatus. ^{1}H and ^{13}C NMR data were obtained using a Bruker Avance 400 MHz spectrometer, with deuterated chloroform ($CDCl_3$) and dimethyl sulfoxide (DMSO-d_6) as the solvent. Chemical shifts (δ) were given as parts per million (ppm) and coupling constants in units of Hertz (Hz). Elemental analyses for C, H and N were carried out on a Thermo Scientific FLASH 2000 CHNS Organic Elemental Analyzer. FTIR spectra were obtained using a Perkin Elmer 100 FTIR Spectrometer with a Gladia ATR Sampling Accessory component. UV–Vis spectra were recorded in the range of 190–1100 nm using a PG model Instruments Ltd., T80 + UV/VIS Spectrophotometer. The single-photon fluorescence spectra were recorded on a Perkin Elmer LS55 spectrofluorophotometer. Spectrophotometric grade DCM was used, and samples were examined using a quartz sample cell of 1 cm optical path. Concentration of samples in DCM was 1.0×10^{-5} molL^{-1}, and a 266 nm excitation wavelength was applied. The respective photoluminescence quantum yields (QYs) were measured using the standard 9,10-diphenylantracene [11–13].

2.3. Calculation of QSAR molecular descriptors

Quantitative Structure-Activity Relationships (QSAR) were gathered to correlate biological activities with physiochemical properties, and were obtained using HyperChem [14]; Molecular Mechanics Force Field (MM+) was used to pre-optimize structures which were refined using the semi-empirical PM3 method. HOMO and LUMO values were computed from the geometry optimized structures.

2.4. General procedure for synthesis of (4-alkyl-1-naphthoylamino)-benzenesulfonamide compounds (**3a–d**)

(4-Alkyl-1-naphthoylamino)-benzenesulfonamides (**6–9**) were synthesized following a slightly modified method of the literature [10], where the modifications used are described below in the text.

2.5. (4-Methyl-1-naphthyl)-quinolin-3-ylamide (**6**)

An orange colored oil formed: yield: 50%. FTIR (ATR): 3475 (NH-secondary amine), 1714, 1627, 1589, 1493 and 1259 (C=O, carbonyl group; C=N, C=C, C–C, C–N, aromatic ring), 1057 (C–N, amide), 2924 (C–H, aromatic ring) 2873 (C–H, alkane), 1441 (CH_2, alkane), 1381 cm^{-1} (CH_3, alkane); UV–Vis (CH_2Cl_2) λ_{max}: 280, 290, 302 nm; ^{1}H NMR (400 MHz, DMSO-d_6 ppm): δ 3.12 (s, 3H, $-CH_3$), 6.88 (s, 1H, N–H), 7.31 (d, J = 7.2 Mz, 1H, Ar–H), 7.40 (d, J = 6.8 Mz, 1H, Ar–H), 7.56–7.63 (m, 8H, Ar–H), 7.72 (d, J = 9.6 Mz, 1H, Ar–H), 8.09 (d, J = 7.2 Mz, 1H, Ar–H); ^{13}C NMR (100 MHz, DMSO-d_6) δ 19.5, 123.9, 125.1, 125.7 (2C), 126.3 (2C), 126.8 (3C), 127.1 (5C), 129.5, 132.4 (2C), 133.8, 135.4, 170.0 (C=O); MS (EI) m/z (relative intensity) 312 (M^+, 100), 197 (10), 183 (82), 170(4), 80 (48); Anal. Calcd. for $C_{21}H_{16}N_2O$: C, 80.75, H, 5.16, N, 8.97, O, 5.12. Found: C, 80.83, H, 5.45, N, 9.02.

2.6. (4-Ethyl-1-naphthyl)-quinolin-3-ylamide (**7**)

An orange colored oil formed: yield: 55%. FTIR (ATR): 2964 (NH-secondary amine), 1705, 1629, 1586, 1493 and 1259, (C=O, carbonyl group; C=N, C=C, C–C, C–N, aromatic ring), 1058 (C–N, amide), 2929 (C–H, aromatic ring) 2872 (C–H, alkane), 1452 (CH_2, alkane), 1397 cm^{-1} (CH_3, alkane); UV–Vis (CH_2Cl_2) λ_{max}: 282, 292, 302 nm; ^{1}H NMR (400 MHz, DMSO-d_6 ppm): δ 1.31 (t, J = 7.4 Mz, 3H, $-CH_3$), 3.10 (q, J = 6.9 Mz, 2H, $-CH_2$), 6.88 (s, 1H, N–H), 7.34 (d, J = 7.2 Mz, 1H, Ar–H), 7.40 (d, J = 7.2 Mz, 1H, Ar–H), 7.54–7.62 (m, 8H, Ar–H), 7.72 (d, J = 7.6 Mz, 1H, Ar–H), 8.14 (d, J = 8.4 Mz, 1H, Ar–H); ^{13}C NMR (100 MHz, DMSO-d_6) δ 15.4, 25.7, 123.9, 124.6, 124.7 (2C), 125.9 (2C), 126.8 (3C), 126.9 (5C), 129.8, 131.6 (2C), 133.8, 141.2, 170.0 (C=O); MS (EI) m/z (relative intensity) 325 ($[M-1]^+$, 100), 183 (99), 119 (35), 80 (46); Anal. Calcd. for $C_{22}H_{18}N_2O$: C, 80.96, H, 5.56, N, 8.58, O, 4.90. Found: C, 81.07, H, 5.84, N, 8.93.

2.7. (4-Propyl-1-naphthyl)-quinolin-3-ylamide (**8**)

An orange colored oil formed: yield: 56%. FTIR (ATR): 2956 (NH-secondary amine), 1707, 1630, 1586, 1494 and 1258 (C=O, carbonyl group; C=N, C=C, C–C, C–N, aromatic ring), 1057 (C–N, amide), 2928 (C–H, aromatic ring) 2869 (C–H, alkane), 1452 (CH_2, alkane), 1381 cm^{-1} (CH_3, alkane); UV–Vis (CH_2Cl_2) λ_{max}: 282, 292, 302 nm; ^{1}H NMR (400 MHz, DMSO-d_6 ppm): δ 0.98 (t, J = 7.2 Mz, 3H, $-CH_3$), 1.68–1.74 (m, 4H, 2[-CH_2]), 6.85 (s, 1H, N–H), 7.33 (d, J = 7.2 Mz, 1H, Ar–H) 7.38 (d, J = 7.2 Mz, 1H, Ar–H), 7.54–7.62 (m, 8H, Ar–H), 7.71 (d, J = 7.6 Mz, 1H, Ar–H), 8.14 (d, J = 7.2 Mz, 1H, Ar–H); ^{13}C NMR (100 MHz, DMSO-d_6) δ 14.4, 24.0, 34.6, 123.8, 124.8, 125.8 (2C), 125.9 (2C), 126.7 (3C), 126.9 (5C), 129.8, 131.8 (2C), 133.8, 139.6, 170.0 (C=O); MS (EI) m/z (relative intensity) 340 (M^+, 100), 197 (10), 183(82), 119 (34), 80 (55); Anal. Calcd. for $C_{23}H_{20}N_2O$: C, 81.15, H, 5.92, N, 8.23, O, 4.70. Found: C, 81.45, H, 6.37, N, 8.49.

2.8. (4-Butyl-1-naphthyl)-quinolin-3-ylamide (**9**)

An orange colored oil formed: yield: 65%. FTIR (ATR): 2953 (NH-secondary amine), 1707, 1632, 1587, 1494 and 1260 (C=O, carbonyl group; C=N, C=C, C–C, C–N, aromatic ring), 1057 (C–N, amide), 2928 (C–H, aromatic ring) 2868 (C–H, alkane), 1458 (CH_2, alkane), 1381 cm^{-1} (CH_3, alkane); UV–Vis (CH_2Cl_2) λ_{max}: 282, 292, 302 nm; ^{1}H NMR (400 MHz, DMSO-d_6 ppm): δ 0.93 (t, J = 7.4 Mz, 3H, $-CH_3$),

1.36–1.45 (m, 4H, 2[-CH_2]), 1.66 (t, J = 7.4 Mz, 2H, $-CH_2$), 6.85 (s, 1H, N–H), 7.32 (d, J = 7.2 Mz, 1H, Ar–H), 7.38 (d, J = 7.2 Mz, 1H, Ar–H), 7.56–7.63 (m, 8H, Ar–H), 7.72 (d, J = 8.0 Mz, 1H, Ar–H), 8.13 (d, J = 6.8 Mz, 1H, Ar–H); ^{13}C NMR (100 MHz, DMSO-d_6) δ 14.3, 22.6, 33.0, 34.6, 123.8, 124.7, 125.7 (2C), 125.9 (2C), 126.7 (3C), 126.9 (5C), 129.8, 131.7 (2C), 133.8, 139.9, 170.0 (C=O); MS (EI) m/z (relative intensity) 355 ([M+1], 8), 278 (100), 101 (7), 57 (9); Anal. Calcd. For $C_{24}H_{22}N_2O$: C, 81.33, H, 6.26, N, 7.90, O, 4.51. Found: C, 81.79, H, 6.59, N, 7.98.

3. Results and discussion

3.1. General properties of 4-alkyl-1-naphthyl)-quinolin-3-ylamide derivatives (**6**–**9**)

The synthesized derivatives were obtained as orange coloured oils and were stable at room temperature. They were miscible with DMF, THF, methanol, ethanol, chloroform and DCM, and immiscible in water. The elemental analyses are given in the materials and method section, and are in good agreement with the calculated values.

3.2. Chemistry

(4-Alkyl-1-naphthyl)-quinolin-3-ylamide derivatives (**6**–**9**) were obtained from 3-aminoquinoline (**5**) and 4-alkylnaphthalene carboxylic acids, following a slightly modified synthetic method of the literature [10]. These modifications entailed the final step of nucleophilic addition/elimination reaction, where the solvent media for the naphthoyl chloride preparation was DMF, rather than DCM, due to solubility complications. Further, removal of the NEM salt by filtration was left to the end, where precipitation of this NEM. HCl salt was initiated by ethyl acetate addition. Drying ($MgSO_4$), concentration by *in vacuo* evaporation, and finally purification by column chromatography yielded the derivatives.

The 4-alkylnaphthoic acids, except for 4-methylnaphthoic acid which was readily available, were synthesized as described in the literature [15]. This series of compounds was developed such that the 4-alkyl carbon length varied in size from the small methyl to the larger butyl group. The synthesis of (4-alkyl-1-naphthyl)-quinolin-3-ylamide derivatives (**6**–**9**) was achieved using the methodology given in Scheme 1.

3.3. Antimicrobial activity

An agar diffusion method with sterile filter paper disks was utilized to detect antimicrobial activity [16]. The following microbes were used: three Gram-positive bacteria (*Bacillus subtilis*, *Bacillus megaterium* and *Staphylococcus aureus*), four Gram-negative bacteria (*Enterobacter aerogenes*, *Escherichia coli* DM, *Klebsiella pneumonia* and *Pseudomonas aeruginosa*) and three yeasts (*Candida albicans*, *Saccharomyces cerevisiae* and *Yarrowia lipolytica*). All microorganisms were obtained from the Department of Biology, Kahramanmaras Sutcu Imam University, Turkey.

The *in vitro* antimicrobial data collection was performed following typical techniques [16]. The test solutions were prepared in methanol. The inhibition zones on media were measured in triplicate, expressed as average values, and given in mm. The antimicrobial activities are given in Table 1.

The derivatives exhibited impressive antimicrobial activities. As a representative example, the photographs of the antimicrobial activity, reflected as inhibition zones of Gram-positive and Gram-negative bacteria (*Staphylococcus aureus* and *Klebsiella pneumoniae*, respectively) for the derivatives (**6**–**9**) and 3-aminoquinoline (**5**) are given in Fig. 1.

The antimicrobial activity observed for all the synthesized derivatives (**6**–**9**), in general, showed greater antimicrobial activity than the precursor compound 3-aminoquinoline (**5**). Antimicrobial data obtained showed that the 4-methyl- analogue (**6**) had somewhat the lowest degree of activity, while the 4-ethyl-, 4-propyl- and 4-butyl- analogues had reasonably high and similar activities; it was the highest for the 4-butyl- analogue (**9**). It was noted the antibacterial activity of both the Gram-positive and Gram-negative bacteria were indistinguisable, but the antifungal activity was less profound for all the compounds. The derivatives (**6**–**9**) had inhibition zones of the range 11–32 mm, whereas the precursor compound (**5**) had a range of 11–13 mm. An examination of the antibacterial and antifungal activities of these derivatives revealed that antimicrobial activity was not restricted to any particular type of microorganism, giving antimicrobial activities against Gram-positive and Gram-negative bacteria and several yeasts.

3.4. Physicochemical data in QSAR studies

QSAR studies of the synthesized derivatives were examined. The

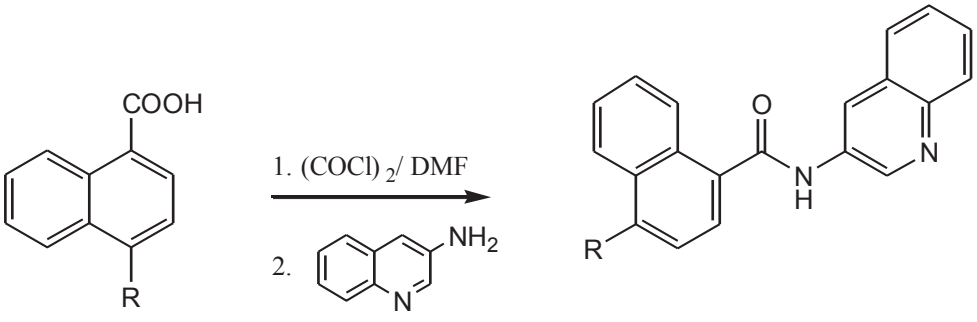

*1 R = CH_3
2 R = C_2H_5
3 R = C_3H_7
4 R = C_4H_9

*5

6 R = CH_3
7 R = C_2H_5
8 R = C_3H_7
9 R = C_4H_9

* Commercially available

Scheme 1. Synthesis of (4-alkyl-1-naphthyl)-quinolin-3-ylamide derivatives.

Table 1
Antimicrobial activity data for (4-alkyl-1-naphthyl)-quinolin-3-ylamide derivatives (**6**–**9**) and 3-aminoquinoline (**5**).

Compound[b]	Microorganism[a]									
	Gr (+)			Gr (−)				Yeast		
	Bacillus Subtilis	*Bacillus megaterium*	*Staphylococcus aureus*	*Enterobacter aerogenes*	*Escherichia coli*	*Klebsiella pneumoniae*	*Pseudomonas aeruginosa*	*Candida albicans*	*Saccharomyces cerevisiae*	*Yarrovia lipolytica*
5	12	11	13	12	11	11	12	–	–	12
6	20	12	26	16	16	18	16	12	13	11
7	28	24	28	24	24	22	18	21	14	12
8	24	28	26	24	22	26	24	14	18	11
9	26	32	24	28	20	24	24	11	19	12

- no activity observed.
[a] % growth inhibition.
[b] Concentration 1,2 mg/per disk.

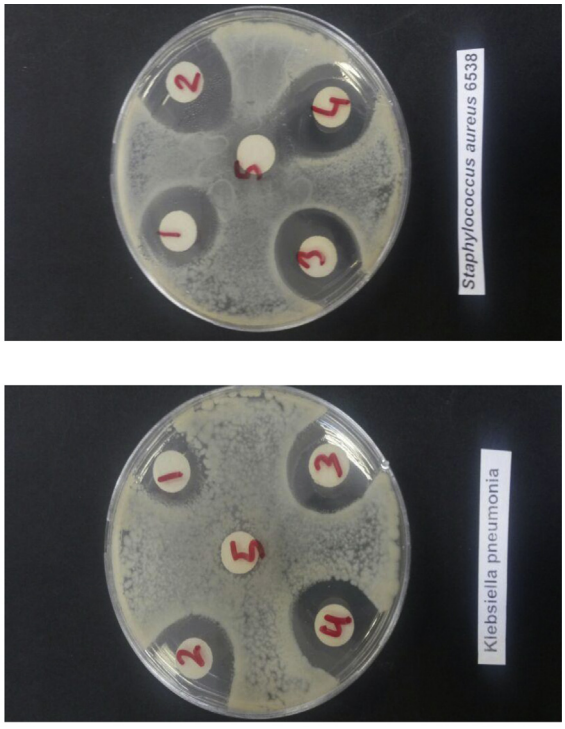

1: (4-methyl-1-naphthyl)-quinolin-3-ylamide (**6**), 2: (4-ethyl-1-naphthyl)-quinolin-3-ylamide (**7**), 3: (4-propyl-1-naphthyl)-quinolin-3-ylamide (**8**), 4: (4-butyl-1-naphthyl)-quinolin-3-ylamide (**9**) 5: 3-aminoquinoline (**5**).

Fig. 1. Inhibition zones of Gram-positive and Gram-negative bacteria (*Staphylococcus aureus* and *Klebsiella pneumoniae*, respectively) for (4-alkyl-1-naphthyl)-quinolin-3-ylamide derivatives (**6**–**9**) and 3-aminoquinoline (**5**).

values of selected descriptors for the new 3-aminoquinoline derivatives are given in Table 2.

The field of QSAR allows us relate the biological activity of a series of compounds to their physicochemical parameters [17–19] Lipophilicity is the physicochemical property widely used in medicinal chemistry, and is designated as the logP value; this is also known as the octanol-water partition coefficient [17–19]. High lipophilic parameters show good permeation of compounds through cell membranes. It can be seen from Table 2 that there were slight increases in lipophilicity from (4-methyl-1-naphthyl)-quinolin-3-ylamide (**6**) through to (4-butyl-1-naphthyl)-quinolin-3-ylamide (**9**), and likewise the antimicrobial activity showed a similar trend, with slight increases in antimicrobial activity. The same pattern was noted with respect to the molecular volume (MV) and molecular refractivity (MR) values, where higher MV and MR values gave greater antimicrobial activities. Chain length increments led to molecular weight (MW) increases as expected. The MW of the precursor compound 3-aminoquinoline (**5**) has a much lower MW than its derivatives. MR increased from the 4-methyl- to 4-butyl- derivatives; compound **5** had the lowest MR value. It can be seen that the log P values also increased from the 4-methyl to 4-butyl derivatives; this is expected as log P is a measure of lipohilicity, and chain length increments of $-CH_2-$ from 4-methyl- to 4-butyl- increase lipohilicity. There was a great change in the energy difference (ΔE) between the HOMO and LUMO of compound **5** compared to its derivatives (**6**–**9**). However, ΔE for the derivatives in general increased slightly with $-CH_2-$ increments from the 4-methyl- to 4-butyl- derivatives. The naphthoyl and quinoline subunits are the unchanged components of the derivatives, thus this may be the main reason for the slight energy differences (ΔE) between HOMO and LUMO of the derivatives. Thus, the 4-alkyl chain lengths, and naphthoyl and quinoline subunits all affected lipophilicity and antimicrobial activity in slightly differing degrees.

3.5. Ultraviolet–Visible spectrophotometer (UV–Vis) measurements

The UV–Vis spectra of the synthesized compounds (**6**–**9**) and the precusor compound 3-aminoquinoline (**5**) were examined in spectrophotometric grade DCM solvent, and are shown in Fig. 2. Spectrophotometric grade DCM solvent was used for the analysis. DCM solvent has a polarity index of 3.1, and two absorptions can be distinguished at 274 and 344 nm for the precursor compound (**5**), and this is in agreement with data given in the literature [20,21]. The absorption at 274 nm is ascribed to the π-π* transition in the

Table 2
Selected QSAR descriptors for the derivatives synthesized, HOMO and LUMO calculated by the PM3 method.

Compound	logP	MW	MV (Å^3)	MR (Å^3)	HOMO (eV)	LUMO (eV)	ΔE (eV)
5	−1.30	144.18	452.87	50.48	−8.174	−0.4112	7.763
6	1.19	312.37	871.69	105.64	−8.984	−0.8317	8.152
7	1.58	326.40	903.09	110.24	−8.988	−0.8317	8.156
8	1.98	340.42	970.96	114.84	−8.984	−0.8324	8.152
9	2.38	354.45	1023.25	119.44	−8.983	−0.8317	8.151

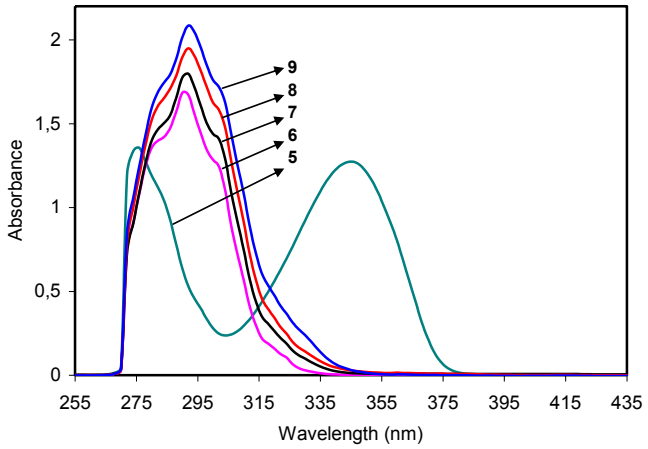

Fig. 2. UV–Vis spectra of (4-alkyl-1-naphthyl)-quinolin-3-ylamide derivatives (**6**–**9**) and 3-aminoquinolin (**5**).

benzenoid ring. The 344 nm absorption describes the n-π* transition in the precursor quinoline ring. Thus, the existence of two peaks in the spectrum of the precursor quinoline ring implicates the presence of two types of chemically nonequivalent rings of the precursor ring structure, specifically, the benzenoid and quinoline rings. Fig. 2 indicates that the 3-aminoquinoline derivatives are in totally different forms due to the absorption band observed, with λ_{max} at 292 nm. In spectra, the absorption at 292 nm is described as the π-π* transition in the benzenoid rings of the 3-aminoquinoline derivatives. Also, the 3-aminoquinoline derivatives showed two large shoulder peaks at 282 and 302 nm, in addition to the main peak at 292 nm. However, the absorption peak observed at 344 nm for 3-aminoquinoline compound disappeared for all the 3-aminoquinoline derivatives. This indicates that there were no n-π* transitions in the 3-aminoquinoline derivatives. In other words, all the electronic energy level transitions converted to π-π* transitions in the 3-aminoquinoline derivatives. It can be seen from the spectra of the 3-aminoquinoline derivatives that the intensity of the π-π* transition peak increased as a result of the formation of larger cyclic structural molecules, compared to that of the precursor compound. The reason for this increase may be because of these organic molecules being structurally more cyclic, and thus are able to donate more π electrons upon the formation of the 3-aminoquinoline derivatives. Thus, these 3-aminoquinoline derivatives have a rich electronic structure, causing a significant increase in the maximum absorption intensity. However, this maximum absorption intensity increase was very small. Also, this maximum absorption intensity increase was due to the longer alkyl chain, acting as a better electron donating group. Further, the maximum absorption wavelength (292 nm) of all the 3-aminoquinoline derivatives shifted to higher absorption wavelengths, compared to the maximum absorption wavelength (274 nm) of the precursor compound. These results indicated that the more cyclic structural organic molecules donated more π bond electrons as for the 3-aminoquinoline derivatives. The increase in number of π bonds of these organic molecules reduced the band gap between the π-π* transition peak, and thus the transition of electrons occurred at lower energies.

The UV–Vis data for the 3-aminoquinoline derivatives (**6**–**9**) and 3-aminoquinoline compound (**5**) are summarized in Table 3. The molar absorptivity coefficient values of all the 3-aminoquinoline derivatives increased as compared to that of the precursor compound. The rich electronic structures of these molecules cause significant increases in the molar absorption capacity for all the 3-aminoquinoline derivatives as compared to the

Table 3
UV–Vis data for (4-alkyl-1-naphthyl)-quinolin-3-ylamide derivatives (**6**–**9**) and 3-aminoquinoline (**5**).

Compound	ε (L mol^{-1} cm^{-1})	λ_{max} Abs (nm)	In Abs
5	6.68×10^4	274	1.336
6	8.42×10^4	290	1.684
7	8.98×10^4	292	1.796
8	9.75×10^4	292	1.950
9	10.43×10^4	292	2.085

λ_{max} Abs: maximum absorption wavelength, In Abs: maximum absorption intensity, ε: molar absorptivity coefficient, sample concentrations: 2.0×10^{-5} mol/L.

precursor compound 3-aminoquinoline. However, this increase in molar absorptivity coefficient values was very small for the 3-aminoquinoline derivatives. These differences in molar absorptivity coefficient values may originate from the slight size differences of the alkyl substituents, while the remaining larger main molecular structures are unchanged. The introduction of better electron donating groups, that is, larger alkyl chains at the para positions, cause extended conjugation, and this is reflected as improved hyperconjugation, and results in increased molar absorptivity coefficients of the derivatives.

3.6. Fourier transform infrared spectroscopy (FTIR) measurements

The FTIR spectra of the synthesized compounds (**6**–**9**) and the precursor compound 3-aminoquinoline (**5**) are shown in Fig. 3. A comparison of 3-aminoquinoline and its derivatives showed that the intensity of all the peaks changed dramatically; the intensity of the peaks for all the derivatives increased, becoming more sharper than that of the 3-aminoquinoline compound. Further, new peaks appeared upon the formation of derivatives, indicating that all the reactions were carried out successfully.

It can be seen from the FTIR spectrum of the compound 3-aminoquinoline (**5**, Fig. 3), that all the expected peaks observed were consistent with the chemical structure of 3-aminoquinoline. For example, the peaks at 3457 and 3323 cm^{-1} belong to the different modes of N–H stretching for the primary amine group (-NH_2) of 3-aminoquinoline [21,22]. The weak peaks at 3190 and 2988 cm^{-1} belong to C–H stretching [21,22]. The aromatic ring

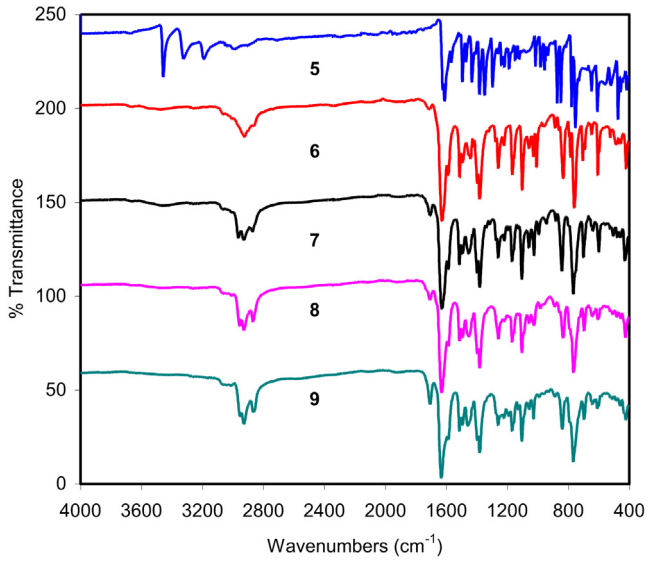

Fig. 3. FTIR spectra of (4-alkyl-1-naphthyl)-quinolin-3-ylamide derivatives (**6**–**9**) and 3-aminoquinoline (**5**).

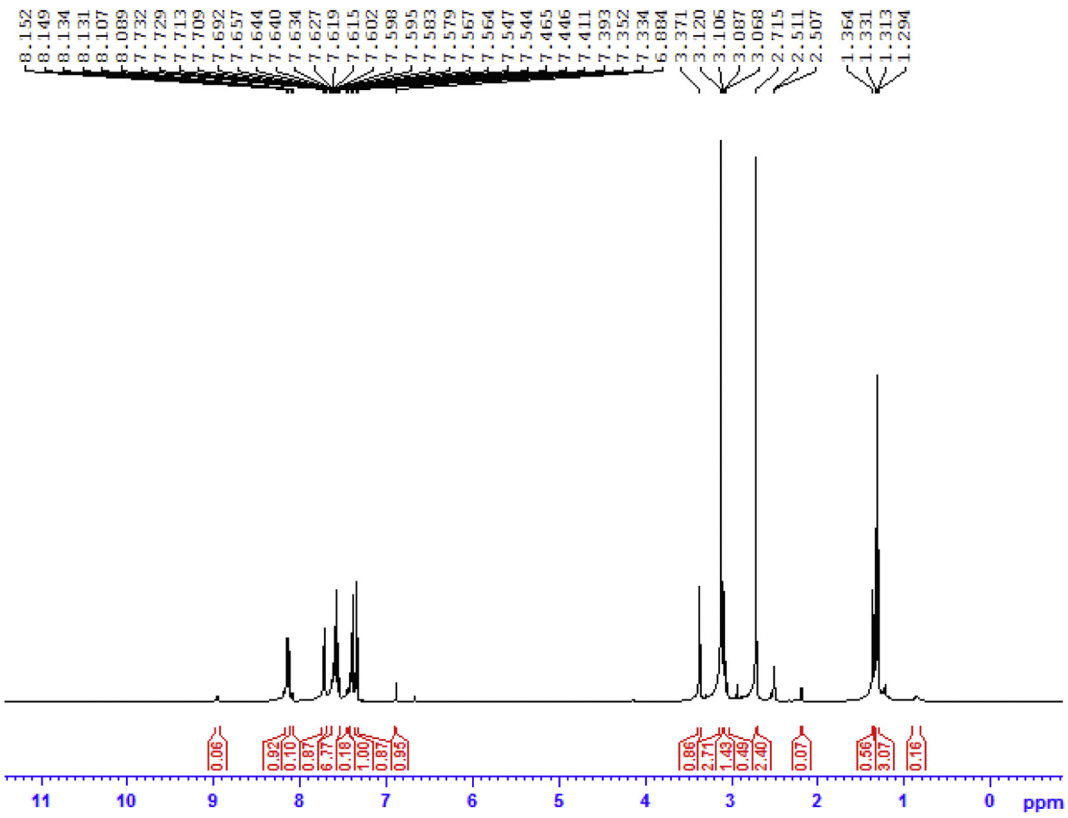

Fig. 4. ^{1}H NMR spectrum of (4-ethyl-1-naphthyl)-quinolin-3-ylamide (**7**).

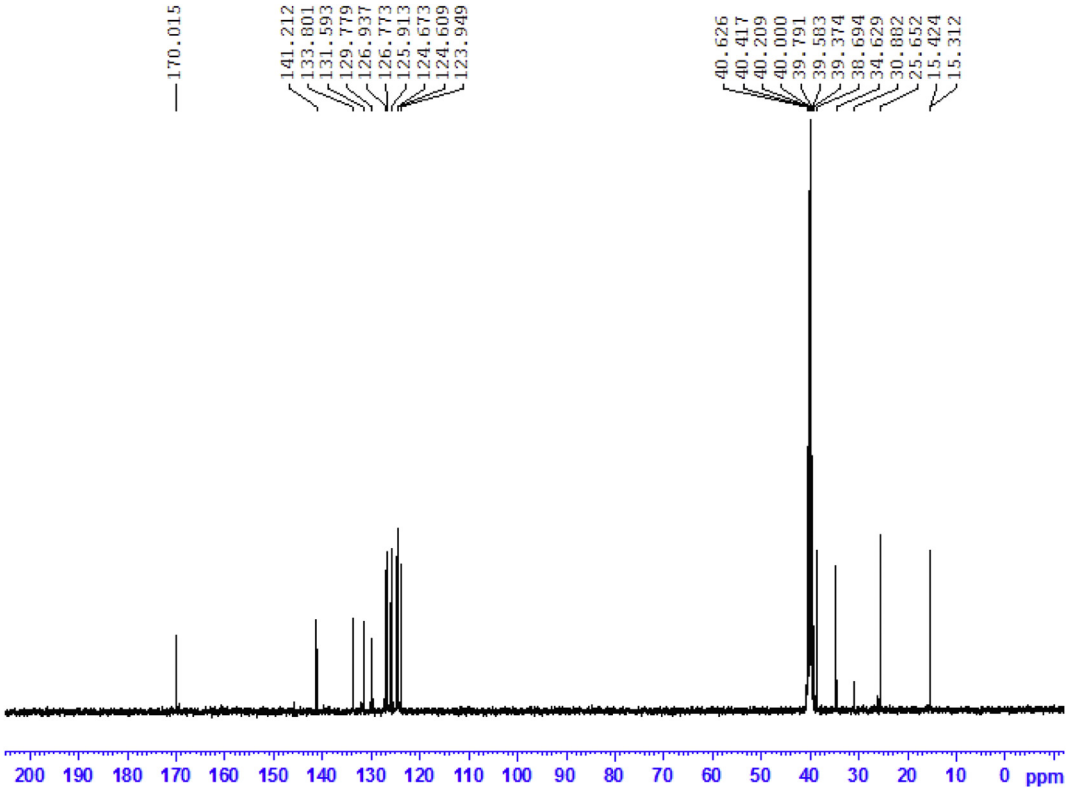

Fig. 5. ^{13}C NMR spectrum of (4-ethyl-1-naphthyl)-quinolin-3-ylamide (**7**).

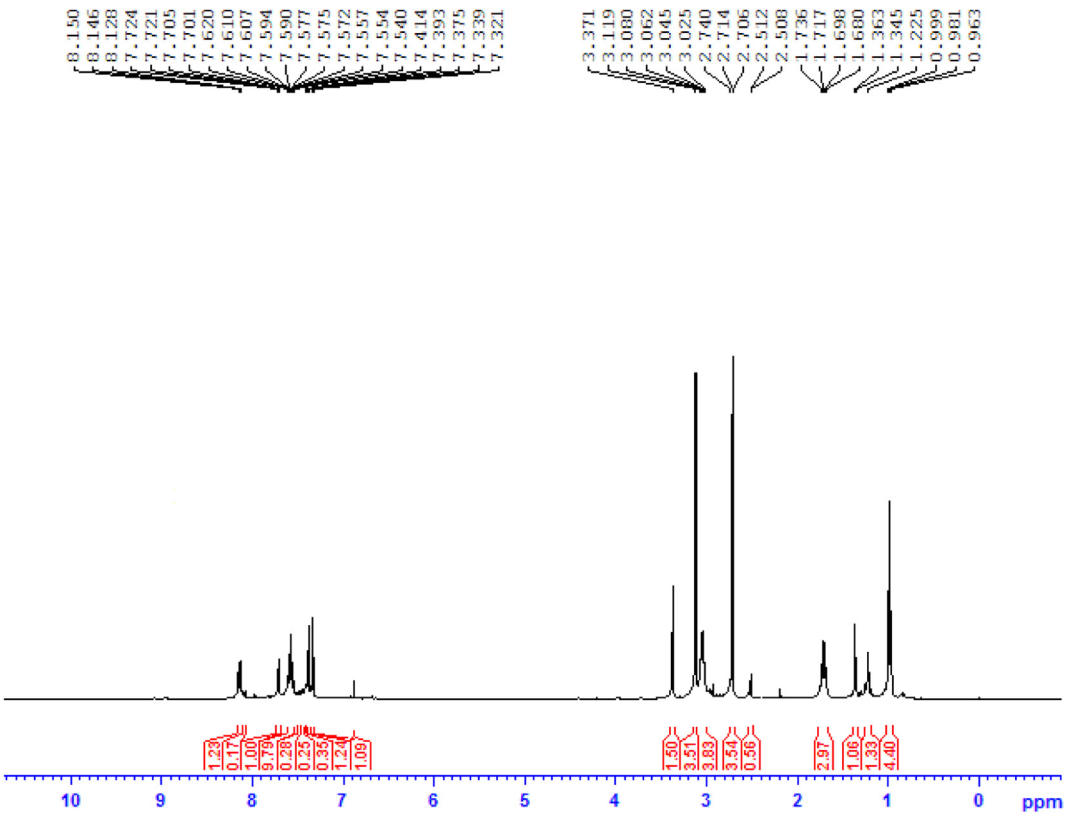

Fig. 6. ^{1}H NMR spectrum of (4-propyl-1-naphthyl)-quinolin-3-ylamide (**8**).

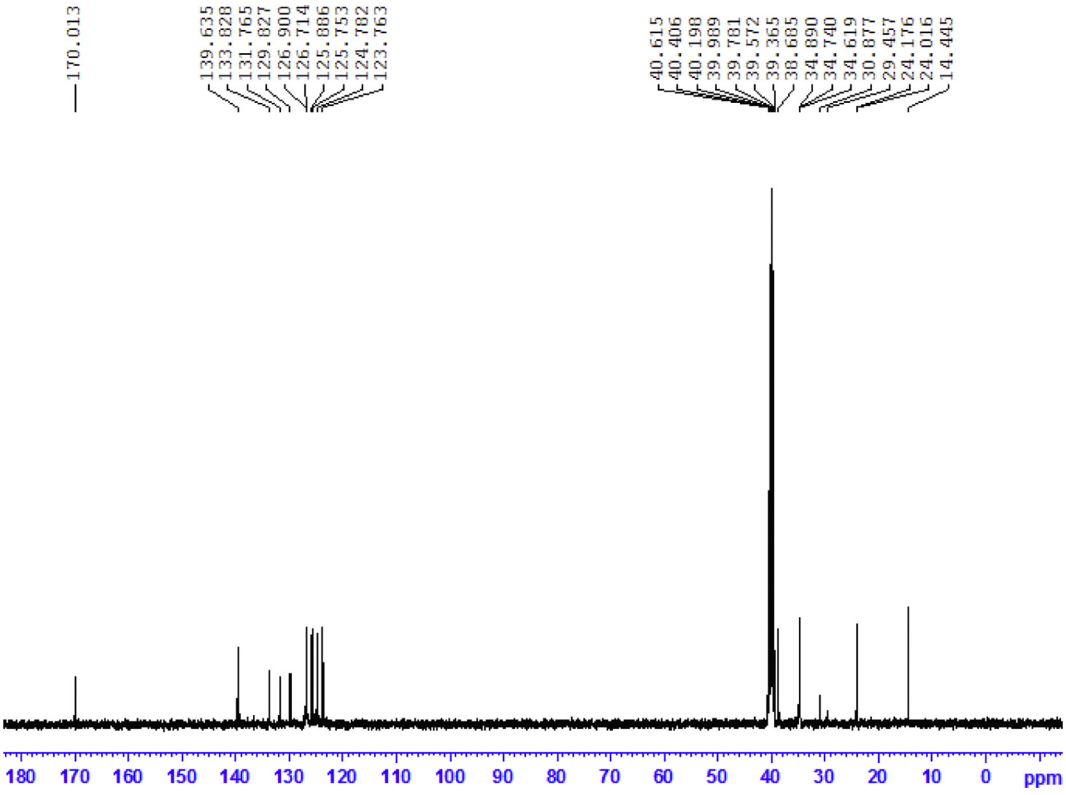

Fig. 7. ^{13}C NMR spectrum of (4-propyl-1-naphthyl)-quinolin-3-ylamide (**8**).

stretching, N–H deformation and the C=C, C–C, C=N and C–N vibrational stretches all give absorptions in the region 1600-1240 cm^{-1}. The strong peaks at about 1219 1188, 1148, 1124 and 1015 cm^{-1} belong to the C–N vibrational stretching between the aromatic ring and primary amine group [21,22].

It can be seen from the FTIR spectra of the 3-aminoquinoline derivatives (**6**–**9**, Fig. 3), that all the expected peaks were observed, and were in accordance with the chemical structures of the 3-aminoquinoline derivatives. The peaks at 3457 and 3323 cm^{-1} belong to the different modes of N–H stretching in the primary amine group (-NH_2) of 3-aminoquinoline (**5**) which disappeared for all the 3-aminoquinoline derivatives (**6**–**9**). The disappearance of these peaks indicated that the primary amine group (-NH_2) of 3-aminoquinoline reacted, and new amide bonds formed, thus being indicative of successful reactions. Further, the mid-strength new peaks appearing at 1707 and 1632 cm^{-1} for all the 3-aminoquinoline derivatives had amide bonds, observed as C=O carbonyl group vibrational stretching in the 3-aminoquinoline derivatives [21,22]. Also, the intensity of the peak at about 1707 cm^{-1} increased upon changing the para substituted methyl group to a butyl alkyl chain. The appearance of these new peaks can be interpreted as additional evidence for new amide bond formation, hence successfully occurring reactions. The mid-strength peaks at 2953 cm^{-1} indicate the different modes of N–H vibrational stretching in the amide group of the 3-aminoquinoline derivatives. The appearance of these new peaks can be accepted as additional evidence for amide bond formation, thus successfully occurring reactions. Further, new peaks also appeared after derivatization, and these peaks can be expressed as below. The peak at about 2928 cm^{-1} belongs to the C–H stretching of the aliphatic

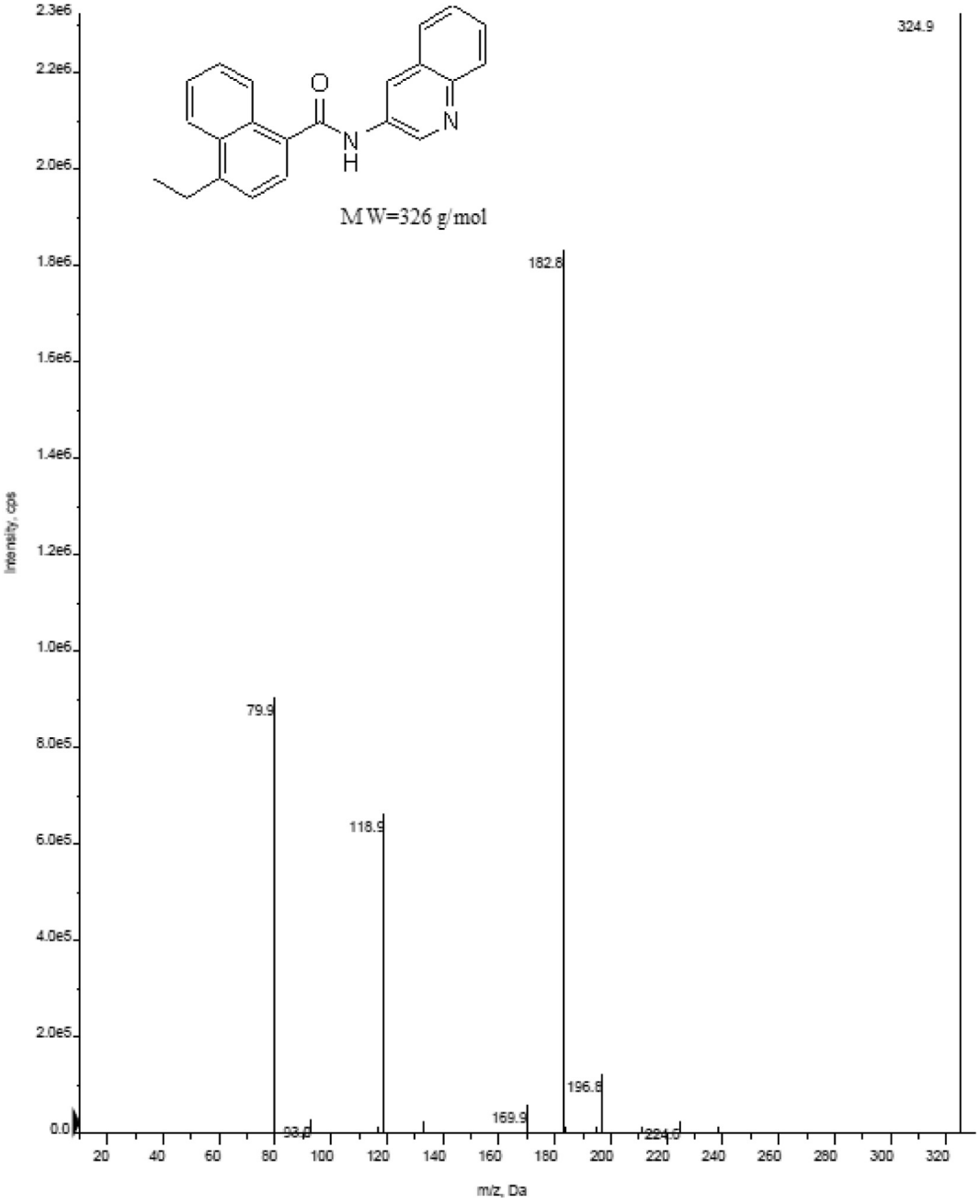

Fig. 8. Mass spectrum of (4-ethyl-1-naphthyl)-quinolin-3-ylamide (**7**).

alkane [21,22]. The peak at about 1458 cm^{-1} belongs to the C–H bending modes of the aliphatic $-CH_2-$ chain. The peak at about 1397 cm^{-1} belongs to the C–H bending modes in the $-CH_3$ chain terminal of the aliphatic structure. The mid-strength peak at 2868 cm^{-1} belongs to the C–H stretching. The aromatic ring stretching, N–H deformation and the C=C, C–C, C=N and C–N vibrational stretches all give absorptions in the region 1600–1240 cm^{-1} [21,22]. The strong peaks at about 1191, 1168, 1128, 1104 and 1057 cm^{-1} belong to the C–N vibrational stretching between the aromatic ring and secondary amine group [21,22]. The region from 1200 to 500 cm^{-1} is the region for the in-plane and out-of-plane bending of C–H bonds of the aromatic rings [21,22]. The main absorption bands for the 3-aminoquinoline derivatives are located at 1027, 888, 839, 767 and 696 cm^{-1}, and some weak bands can be seen. The peaks at about 888, 839, 767 and 696 cm^{-1} are for the C–H out-of-plane bending modes, in particular, para substitution being observed with the peak at 767 cm^{-1}. This is ascribed as the out-of-plane C–H bending. This peak shifted slightly from 760 cm^{-1} to 767 cm^{-1}, from the para substituted methyl group through to the butyl chain. The bands at about 609, 511 and 486 cm^{-1} are the aromatic ring deformation peaks. The medium and strong absorption modes at about 1027, 641 and 460 cm^{-1} belong to the C–H vibrational stretching of the aromatic ring or Ar–H cyclic structure [21,22].

3.7. Nuclear magnetic resonance spectroscopy (^1H and ^{13}C NMR)

^1H and ^{13}C NMR spectra for the synthesized (4-alkyl-1-naphthyl)-quinolin-3-ylamide derivatives (**6**–**9**) were recorded, and the data obtained are given in the materials and method

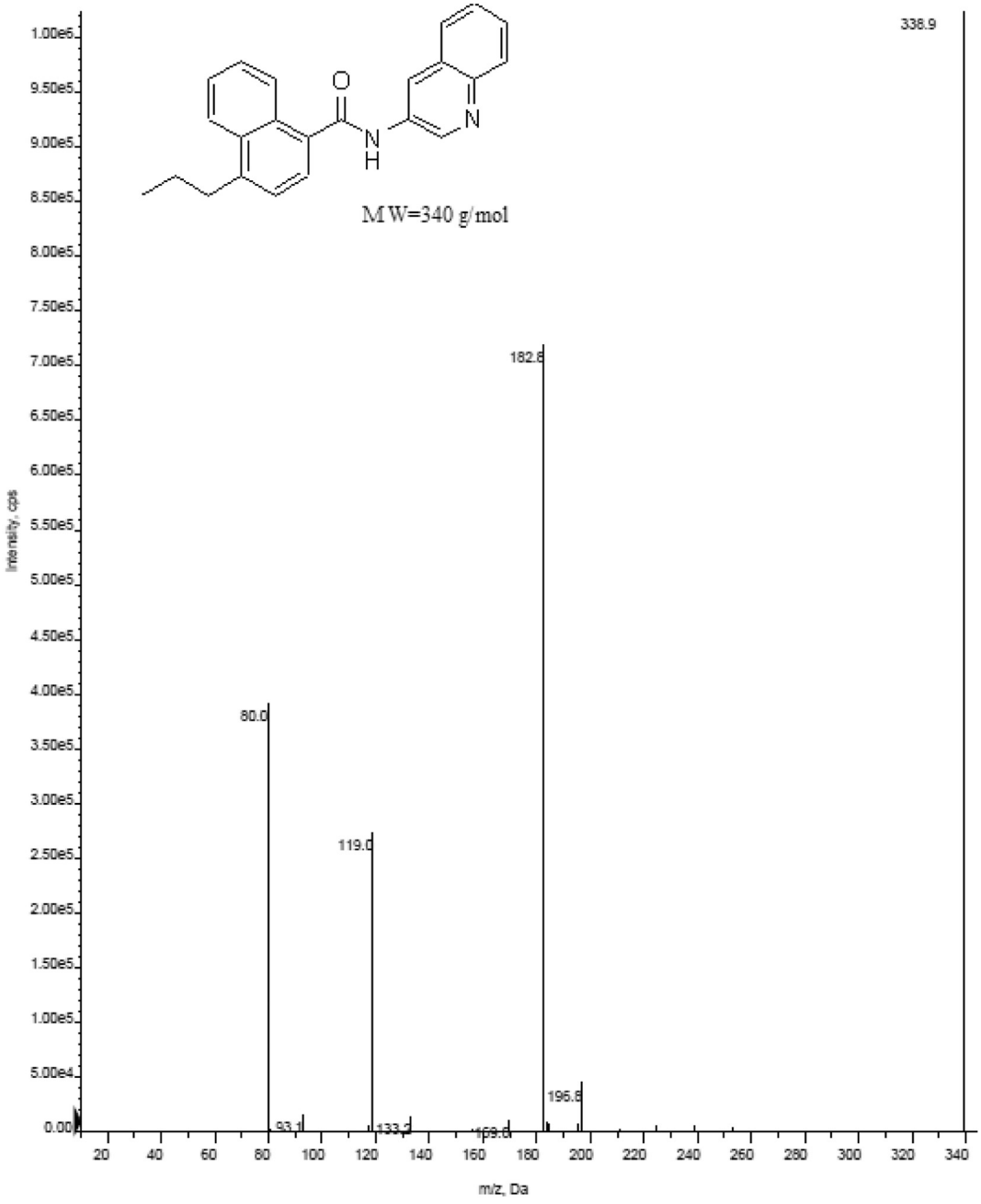

Fig. 9. Mass spectrum of (4-propyl-1-naphthyl)-quinolin-3-ylamide (**8**).

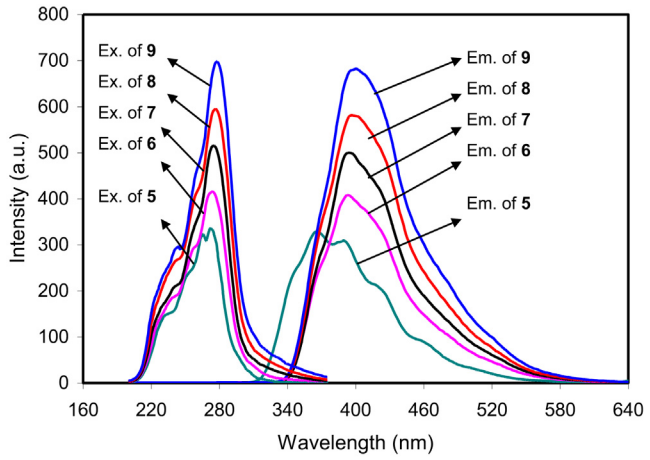

Fig. 10. Photoluminescence spectra of (4-alkyl-1-naphthyl)-quinolin-3-ylamide derivatives (**6**–**9**) and 3-aminoquinoline (**5**) in DCM; samples were excited at 266 nm.

section. As representative examples, the NMR spectra of derivatives **7** and **8** are given in Figs. 4–7. In the ^{1}H NMR spectra of the derivatives, the aliphatic protons were observed in the region δ 0.92–3.12 ppm, and the aromatic protons in the region δ 7.30–8.15 ppm, as commonly given in the literature [21]. The region δ 7.54–7.64 ppm shows an overlapping multiplet, representing the aromatic protons of both the naphthyl and quinoline rings. There are four doublets representing four aromatic C–H protons of the naphthyl and quinoline rings. The two singlets expected for two quinoline C–H protons are probably masked by other low field naphthyl and quinoline C–H protons. The quinoline N–H proton was observed as a singlet about at 6.85 ppm.

In the ^{13}C NMR spectra of the derivatives the aliphatic carbons were observed at δ 14.2–34.6 ppm and the aromatic carbons were observed at δ 123.7–170.0 ppm, as commonly given in the literature [21]. Several carbon signals had exactly the same NMR signal, either as a result of symmetry or by coincidence. In general, carbons having hydrogens are observed as larger peaks than those carbons without hydrogens [21].

3.8. Mass spectra (LC-MS-MS)

The mass spectra for the synthesized (4-alkyl-1-naphthyl)-quinolin-3-ylamide derivatives (**6**–**9**) were recorded, and the data obtained are given in materials and method section. All spectra observed were in accordance with the molecular structures of the compounds. The molecular ions $[M]^+$ of the derivatives were observed as $[M-1]^+$or $[M+1]^+$.

As representative examples, the mass spectra of derivatives **7** and **8** are given in Figs. 8 and 9, respectively. The molecular ion peak $[M-1]^+$ for derivative **7** was observed at m/z 325, while the highest intensity peaks for the derivative was observed at m/z 325 and 183 (100 and 99%, respectively). The m/z 183 fragment of 99% intensity reveals that the predominant decomposition pathway was α-cleavage [23], with the formation of the corresponding acylium cation fragment ($[C_{12}H_{11}C{\equiv}O{:}]^+$, m/z 183), via loss of the quinolin-3-ylamino alkyl group ($[C_9H_7N_2]^{\cdot}$, m/z 143). The molecular ion peak $[M-1]^+$ for derivative **8** was observed at m/z 339, with the highest intensity peaks observed at m/z 339 and 183 (100 and 82%, respectively). Derivative **8** gave the m/z 197 fragment, indicating an α-cleavage decomposition pathway [23], with the formation its corresponding acylium cation fragment ($[C_{13}H_{13}C{\equiv}O{:}]^+$, m/z 197), via loss of the quinolin-3-ylamino alkyl group ($[C_9H_7N_2]^{\cdot}$, m/z 143). All the derivatives seemed to follow the α-cleavage decomposition pathway except for derivative **9**, which seemed to follow a different pattern of decomposition. This may be because it being a more larger and labile structure than the other derivatives (**6**–**8**). Derivative **9** gave the molecular ion peak $[M+1]^+$ at m/z 355 (8%), with the highest intensity peak for the derivative being observed at m/z 278 (100%).

3.9. Photoluminescence measurements

Photoluminescence is an invaluable tool regularly used in medicinal science. Photophysical properties of the compounds synthesized were examined for possible uses in medical imaging. The excitation and emission spectra for (4-alkyl-1-naphthyl)-quinolin-3-ylamide derivatives (**6**–**9**) and 3-aminoquinoline (**5**) solutions were studied, with excitation at 266 nm.

3-Aminoquinoline (**5**) showed weak emission, while its derivatives gave an intense emission upon irradiation by UV light. The photoluminescence spectra of these compounds are shown in Fig. 10. A weak maximum luminescent intensity was observed at 366 nm. The full width at half maximum (FWHM) was 93 nm for compound 3-aminoquinoline (**5**). Compound 3-aminoquinoline (**5**) revealed 18% QY and 1.70 ns lifetime of the excited-state. Maximum emission was observed at 396 nm and the FWHM was 74 nm for (4-methyl-1-naphthyl)-quinolin-3-ylamide (**6**). Compound (4-methyl-1-naphthyl)-quinolin-3-ylamide (**6**) revealed 22% QY and 2.05 ns lifetime of the excited-state. The luminescence intensity of the peaks and the QYs of (4-alkyl-1-naphthyl)-quinolin-3-ylamides (**6**–**9**) increased significantly compared to that of the precursor compound 3-aminoquinoline (**5**) as a result of more bulkier cyclic molecules. Further, attachments of more electron donating groups onto the rings at the para-position of the derivatives leads to extended conjugation, and thus improved hyperconjugation, and this results in increased intensities of the main peaks, shifting to greater wavelengths of emission. High QY is a result of extensive π-electron delocalization in large molecular structural systems. Therefore, as a result increasing π bonds or electron rich cyclic molecular systems, the fluorescence emission intensity increases; cyclic molecular systems increase electron delocalization and/or energy transfer from the excited state of the (4-alkyl-1-naphthyl)-quinolin-3-ylamide. This leads to an increase in the non-radiated transition of the (4-alkyl-1-naphthyl)-quinolin-3-ylamide excited state, and an increase in fluorescence emission.

Table 4
Photoluminescence data for (4-alkyl-1-naphthyl)-quinolin-3-ylamide derivatives (**6**–**9**) and 3-aminoquinoline (**5**).

Compound	λ_{max} Ex (nm)	In Ex	$_{max}$ Em (nm)	In Em	ϕ_f (%)	τ_f (ns)
5	274 (230; 248; 263; 281)	332	366 (348; 393; 425; 464)	326	18	1.70
6	276 (235; 254; 285)	411	396 (366; 426; 467)	403	22	2.05
7	278 (241; 259; 287)	506	398 (371; 427; 469)	496	26	2.44
8	279 (244; 261; 289)	589	401 (368; 429; 472)	577	30	2.76
9	280 (246; 262; 292)	692	404 (371; 432; 478)	678	34	3.15

λ_{max} Ex: maximum excitation wavelength; In Ex: maximum excitation intensity.
λ_{max} Em: maximum emission wavelength; In Em: maximum emission intensity.
ϕ_f: quantum yield; τ_f: excited-state lifetime.

The photoluminescence data for (4-alkyl-1-naphthyl)-quinolin-3-ylamides (**6**–**9**) and 3-aminoquinoline (**5**) are summarized in Table 4. The luminescene properties of these derivatives may provide great potential for numerous optical applications and for medicinal biomarkers.

4. Conclusion

The synthesis of (4-alkyl-1-naphthyl)-quinolin-3-ylamide derivatives was described. The chemical structures of these compounds were confirmed by FTIR, NMR and MS spectral analyses. The photoluminescence study of the synthesized derivatives showed higher photoluminescence intensities and efficiencies than that of the precursor compound. Emission intensity of the derivatives increased with increasing π bonds as is the case for large molecules, or with the formation of electron rich cyclic systems. QSAR studies, to include the HOMO and LUMO parameters, were employed to reveal the effects of lipophilicity on their *in vitro* antimicrobial activities. The partiton coefficient log P was found to be related to the antimicrobial activity of these compounds, where increases in lipophilicity led to greater antimicrobial effects. The antimicrobial activity of the synthesized derivatives revealed that activities were not restricted to any particular type of microorganism, giving antimicrobial activities against Gram-positive and Gram-negative bacteria and several yeasts. All derivatives had antimicrobial superior to that of the precursor compound. Both the quinoline ring and substituted naphthalene group appeared to play an important role on antimicrobial activities. These derivatives have carbonyl functional groups that may facilitate hydrogen bonding with important cellular units, and thus cause the disturbance and breakdown of normal cellular pathways. Further, these compounds have high lipophilic character and can implicate improved penetration through the outer membranes of harmful microorganisms.

Acknowledgements

The authors would like to thank Gaziantep University for providing the financial support (Project No: FEF.11.07) and Prof. Dr. Metin Dığrak at Kahramanmaras Sutcu Imam University for his help in determining the antimicrobial activity.

References

[1] E.G. Brain, F.P. Doyle, M.D. Mehta, D. Miller, J.H.C. Nayler, E.R. Stove, Derivatives of 6-aminopenicillanic acid. Part IV. Analogues of 2,6 dimethoxyphenylpenicillin in the naphthalene and quinoline series, J. Chem. Soc. (1963) 491–497.
[2] C. Vittorio, B. Guyen, Y. Opoku-Boahen, J. Mann, S.M. Gowan, M. Lloyd, B.R. Martin, N. Stephen, A novel inhibitor of human telomerase derived from 10H-indolo-[3,2-b] quinoline, Bioorg. Med. Chem. Lett. 10 (2000) 2063–2066.
[3] C. Manera, M.G. Cascio, V. Benetti, M. Allara, T. Tuccinardi, A. Martinelli, G. Saccomanni, E. Vivoli, C. Ghelardini, V. Di Marzo, P.L. Ferrarini, New 1,8-naphthyridine and quinoline derivatives as CB2 selective agonists, Bioorg. Med. Chem. Lett. 17 (23) (2007) 6505–6510.
[4] R.S. Upadhayaya, J.K. Vandavasi, R.A. Kardile, S.V. Lahore, S.S. Dixit, H.S. Deokar, P.D. Shinde, M.P. Sarmah, J. Chattopadhyaya, Novel quinoline and naphthalene derivatives as potent antimycobacterial agents, Eur. J. Med. Chem. 45 (5) (2010) 1854–1867.
[5] A. Matteelli, A.C.C. Carvalho, K.E. Dooley, A. Kritski, TMC207: the first compound of a new class of potent anti-tuberculosis drugs, Future Microbiol. 5 (6) (2010) 849–858.
[6] Z. Ates-Alagoz, N. Altanlar, E. Buyukbingol, Synthesis and antimicrobial activity of new tetrahydro-naphthalene-thiazolidinedione and thiohydantoine derivatives, J. Heterocycl. Chem. 46 (6) (2009) 1375–1379.
[7] R.S. Gouhar, M. Youns, Novel series of substituted heterocycles derived from α,β–unsaturated ketones for anticancer evaluation, Res. J. Pharm. Biol. Chem. Sci. 5 (2) (2014) 680–692.
[8] Y. Xia, Z.Y. Yang, P. Xia, K.F. Bastow, Y. Tachibana, S.C. Kuo, E. Hamel, T. Hackl, K.H. Lee, Antitumor agents. 181. Synthesis and biological evaluation of 6,7,2′,3',4'-substituted-1,2,3,4-tetrahydro-2-phenyl-4-quinolones as a new class of antimitotic antitumor agents, J. Med. Chem. 41 (1998) 1155–1162.
[9] L.C. Chou, M.T. Tsai, M.H. Hsu, S.H. Wang, T.D. Way, C.H. Huang, H.Y. Lin, K. Qian, Y. Dong, K.H. Lee, L.J. Huang, S.C. Kuo, Design, synthesis, and preclinical evaluation of new 5, 6- (or 6, 7-) disubstituted-2-(fluorophenyl)quinolin-4-one derivatives as potent antitumor agents, J. Med. Chem. 53 (2010) 8047–8058.
[10] G. Zengin, Z. Nalbantbasi, H. Zengin, H. Turkmen, Synthesis and characterization of cannabimimetic aminoalkylindole based 5-(4-alkyl-1-naphthoylamino)-1,3,4-thiadiazole-2-sulfonamides, Heteroat. Chem. 22 (6) (2011) 707–714.
[11] G.G. Guilbault (Ed.), Practical Fluorescence, Marcel Dekker, New York, USA, 1990.
[12] A. Gilbert, J. Bagott, Essentials of Molecular Photochemistry, CRC Press Boca Raton Inc., Florida, 1991.
[13] J.A. Osaheni, S.A. Jenekhe, Electroactive and photoactive rod-coil copolymers-design, synthesis, and supramolecular regulation of photophysical properties, J. Am. Chem. Soc. 117 (7) (1995) 7389–7398.
[14] HyperChem 7.5 Program, Hypercube Inc., 2002 anadaToronto, C.
[15] J.W. Huffman, G. Zengin, M.-J. Wu, J.Z. Lu, G. Hynd, K. Bushell, A.L.S. Thompson, S. Bushell, C. Tartal, D.P. Hurst, P.H. Reggio, D.E. Selley, M.P. Cassidy, J.L. Wiley, B.R. Martin, Structure–activity relationships for 1-alkyl-3-(1-naphthoyl)indoles at the cannabinoid CB_1 and CB_2 receptors: steric and electronic effects of naphthoyl substituents. New highly selective CB2 receptor agonists, Bioorg. Med. Chem. 13 (2005) 89–112.
[16] C.H. Collins, P.M. Lyne, J.M. Grange, Microbiological Methods, sixth ed., Butterworths, London, 1989, p. 410.
[17] C. Hansch, A quantitative approach to biochemical structure-activity relationships, Act. Chem. Res. 2 (1969) 232–239.
[18] C. Hansch, A. Leo, Q.S.A.R. Exploring, Fundamentals and Application in Chemistry and Biology, American Chemical Society, Washington, DC, USA, 1995, pp. 311–324.
[19] A. Leo, C. Hansch, D. Elkins, Partition coefficients and their uses, Chem. Rev. 71 (6) (1971) 525–616.
[20] E.S. Sales, J.M.F.M. Schneider, M.J.L. Santos, A.J. Bortoluzzi, D.R. Cardoso, W.G. Santos, A.A. Merlo, Quinolines by three-component reaction: synthesis and photophysical studies, J. Braz. Chem. Soc. 26 (3) (2015) 562–571.
[21] G.M. Lampman, D.L. Pavia, G.S. Kriz, J.R. Vyvyan, Spectroscopy, International Edition, fourth ed., 2010.
[22] D.A. Skoog, F.J. Holler, S.R. Crouch, Principles of Instrumental Analysis, sixth ed., Brooks/Cole, Belmont, CA, USA, 2007.
[23] K.P.C. Vollhardt, N.E. Schore, Organic Chemistry: Structure and Function, fifth ed., W.H. Freeman and Company, New York, USA, 2007, pp. 770–772.